

Functionalization of Carbon Fibers with Nitrogen and Oxygen as High Performance Supercapacitor

Kun Luo, Min Zhu, Yuzhen Zhao and ZhihongLuo*

Guangxi Key Laboratory of Universities for Clean Metallurgy Comprehensive Utilization of Nonferrous Metal Resource, College of Materials Science and Engineering, Guilin University of Technology, Guilin, 541004, PR China

Received: August 24, 2017, Accepted: September 25, 2017, Available online: November 06, 2017

Abstract: Functionalization of carbon materials with heteroatom is highly desirable for high-performance supercapacitor applications. Here, a combined method is used to prepare nitrogen and oxygen co-doped carbon fibers by acidification and N₂ cold plasma treatment. Oxygen groups are introduced by acidification, and N₂ groups are introduced by N₂ cold plasma treatment mainly, moreover, acidification and plasma treatment time promote the increase of nitrogen content. The functionalized CFs obtained by acidification and plasma treatment for 60 min has high nitrogen (4.23 at.%) and oxygen (17.48 at.%) content, which shows high specific capacitance (190 F g⁻¹ at 0.2 A g⁻¹) and good cycling stability with maintaining about 83% of initial capacitance after 4000 cycles.

Keywords: Cold plasma, Oxygen groups, Nitrogen groups, Carbon fibers, Supercapacitors

1. INTRODUCTION

Supercapacitors attract growing attentions because they possess higher power density than batteries and higher energy densities than conventional dielectric capacitors. There are two varieties of supercapacitors based on the charge storage mechanism: surface ion adsorption (electrochemical double-layer capacitor, EDLC) and Faradic reactions (pseudocapacitance). Metal oxides and conductive polymer with high capacity and energy density are main electrode materials for pseudocapacitor, however, the conductivity and electrochemical stability is poor. Carbon materials with high conductivity and power density are common electrode materials for EDLC, the long life stability over large voltage range make them attractive for commercial energy storage applications. However, the specific capacitance and energy density of carbon materials is low [1-4]. Recently, growing interests are focused on improving the energy density of carbon materials.

It is reported that functionalization of carbon materials is an effective way to enhance the supercapacitive performance. Hetero atoms doping is one of the most widely used methods to functionalize carbon materials. Among which, nitrogen- and oxygen-containing surface groups can introduce Faradaic reactions, which increase the specific capacitance and energy density of carbon

materials[5-8]. The previous researches demonstrate that the supercapacitive performance of graphene[9-10], carbon nanotubes[11-12] and porous carbon[13-15] has been significantly improved due to the incorporation of nitrogen groups.

Acid treatment is able to dope large amount of oxygen groups, such as carboxyl, carbonyl and hydroxyl, which is commonly used to functionalize carbon nanotube and graphene. Ball milling, thermal annealing, arc-discharge, plasma and etc is used to dope carbon materials with nitrogen in the existence of nitrogen source[16]. The doping process of ball milling is difficult to control, thermal annealing need high temperature, while arc-discharge requires high voltage or current. Plasma treatment is a green method which needs short reaction time and low power consumption, and the incorporated nitrogen content is relatively high. Park and co-workers found that the nitrogen content can approach to 19.7% by using N₂ plasma[17]. However, high voltage and/or vacuum environment is needed. Cold plasma is carried out at low voltage, normal temperature and pressure without serious destruction of carbon materials structure[18-20].

Carbon fibers with low cost are widely used as matrix for electrode materials with high conductivity and mechanical strength, which are promising supercapacitor electrode materials. Here, a combined method was adopted to increase supercapacitive performance of carbon fibers, which is seldom reported. The N, O co-doped carbon fibers was prepared by using acid treatment and N₂

*To whom correspondence should be addressed: Email: luozhihong615@163.com

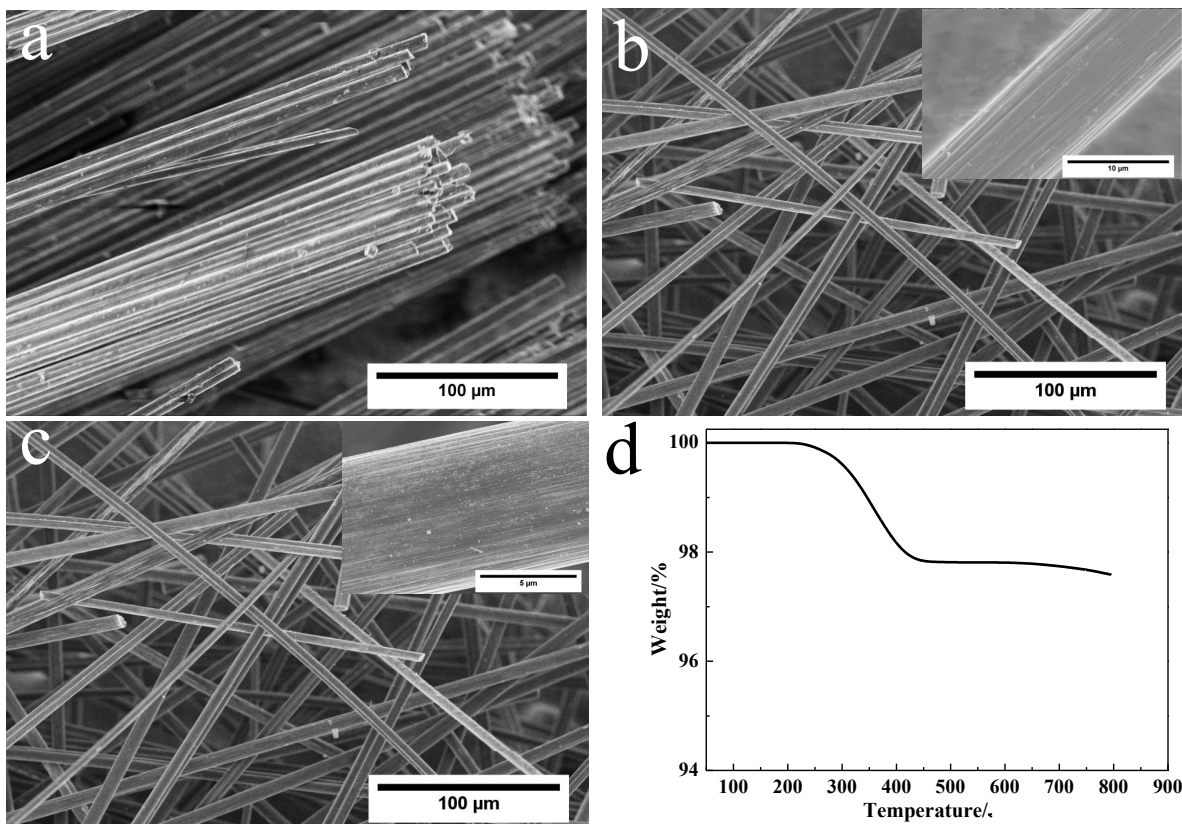


Figure 1. The morphology of pristine CFs (a), T-CFs (b), CFs-60 (c) and TGA plot (d), inset of b and c is the enlarged morphology of T-CFs and CFs-60, respectively.

cold plasma treatment. We find out that acid treatment not only incorporate O groups, but also promote the increase of nitrogen doping efficiency. With acid treatment, the content of nitrogen groups of CFs introduced by cold plasma is higher than the samples without acid treatment, as well as the specific capacitance.

2. EXPERIMENTAL

2.1. Chemicals and Materials

Commercial carbon fibers (CFs, SU350) which comprise individual fiber with diameter of about 7 μm were received from Tenax company. The as-received carbon fibers were heated at 700 $^{\circ}\text{C}$ in Ar atmosphere for 1 h to remove the polymer binders on the surface of CFs, which was named as T-CFs. N_2 with the purity of 99.9% was used, and all chemical reagents were used as received.

2.2. Acidification of CFs

The T-CFs were acidified in concentrated $\text{H}_2\text{SO}_4/\text{HNO}_3$ (v/v 3/1) at 60 $^{\circ}\text{C}$ for 2 h, then washed with distilled water until the filtered water was neutral and dried at 60 $^{\circ}\text{C}$ for 24 h, which were named as A-CFs.

2.3. Microwave treatment of CFs

A-CFs were treated with 700 W for 8 s in a domestic microwave oven, and the obtained CFs were named as M-CFs.

2.4. Functionalization of CFs by non-thermal plasma

A home-made device for generating cold plasma was used to functionalize the M-CFs. A chamber in which a conductive Cu wire was placed was wrapped by tinfoil. One electrode of plasma generator was connected to the Cu wire and another one connected to the tin foil. N_2 flow (1 L min^{-1}) injected into the chamber was blew the M-CFs and excited by voltage of 55 V with the power of 12 W, the power was turn off in every other 2 min to allow the chamber cool down, the plasma treatment was last for 30 min, 60 min and 90 min, and the functionalized CFs were named as CFs-30, CFs-60 and CFs-90, respectively. The carbon fibers without acidification treated by cold plasma N_2 for 60 min were named as T-CFs-60.

2.5. Characterizations

The morphology of the CFs samples was examined by Field emission scanning electron microscopy (FE-SEM, Hitachi, S-4800). Raman spectra were recorded on a Thermo Fisher DXR Raman spectrometer equipped with a 532 nm incident laser light source. The element composition of the samples was determined by an X-ray photoelectron spectroscopic instrument (ESCALAB250Xi, Thermo). The carbon fibers, PTFE and carbon black were mixed with weight ratio of 85: 10: 5, a small amount of

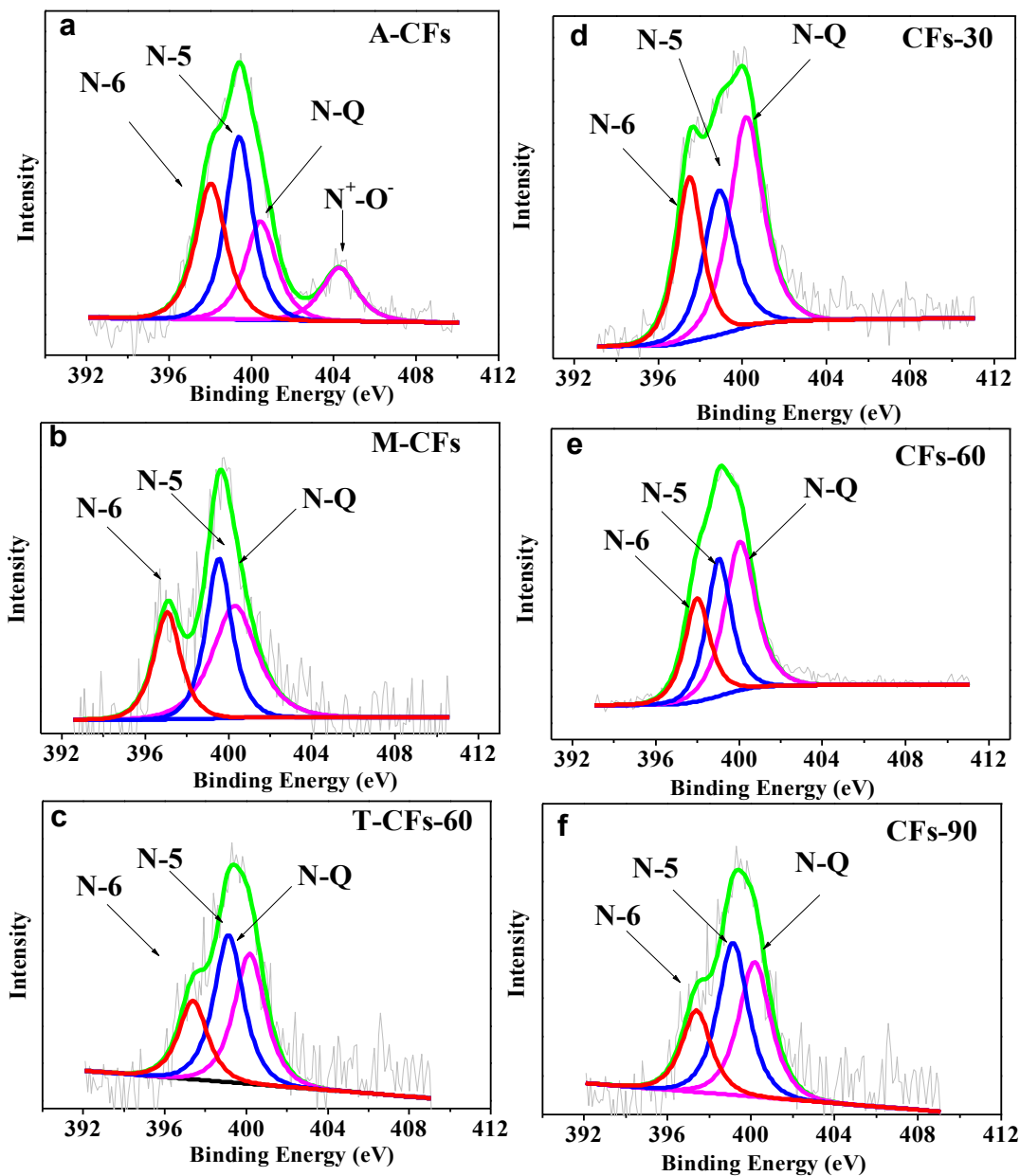


Figure 2. N1s (a, b, c, d, e, f) spectra of A-CFs (a), M-CFs (b), T-CFs-60 (c), CFs-30 (d), CFs-60 (e) and CFs-90 (f)

Table 1. Content of O and N in the A-CFs, M-CFs, CFs-15, CFs-30, CFs-45 and CFs-60

Samples	C at. %	N at. %	O at. %
T-CFs	99.04	ND	0.96
A-CFs	79.83	1.79	18.38
M-CFs	86.59	0.9	12.51
CFs-30	85.26	1.87	12.87
CFs-60	78.29	4.23	17.48
CFs-90	76.51	5.43	18.07
T-CFs-60	86.15	1.30	12.56

ND represented that the element was not detected.

ethanol was added to form the slurry which was pressed onto the foam nickel (1 cm × 1 cm) for electrochemical measurement. All electrochemical analyses were performed on an electrochemical workstation (CHI690, CH Instruments) in a three-electrode setup with 6 mol L⁻¹ KOH as electrolyte, a Pt foil and a saturated calomel electrode (SCE) were used as counter and reference electrode, respectively.

3. RESULTS AND DISCUSSIONS

3.1. Characterization of CFs

In order to enhance the efficiency of functionalization, the polymer binder (about 2.2 wt.% which is measured by TGA, Figure 1d)

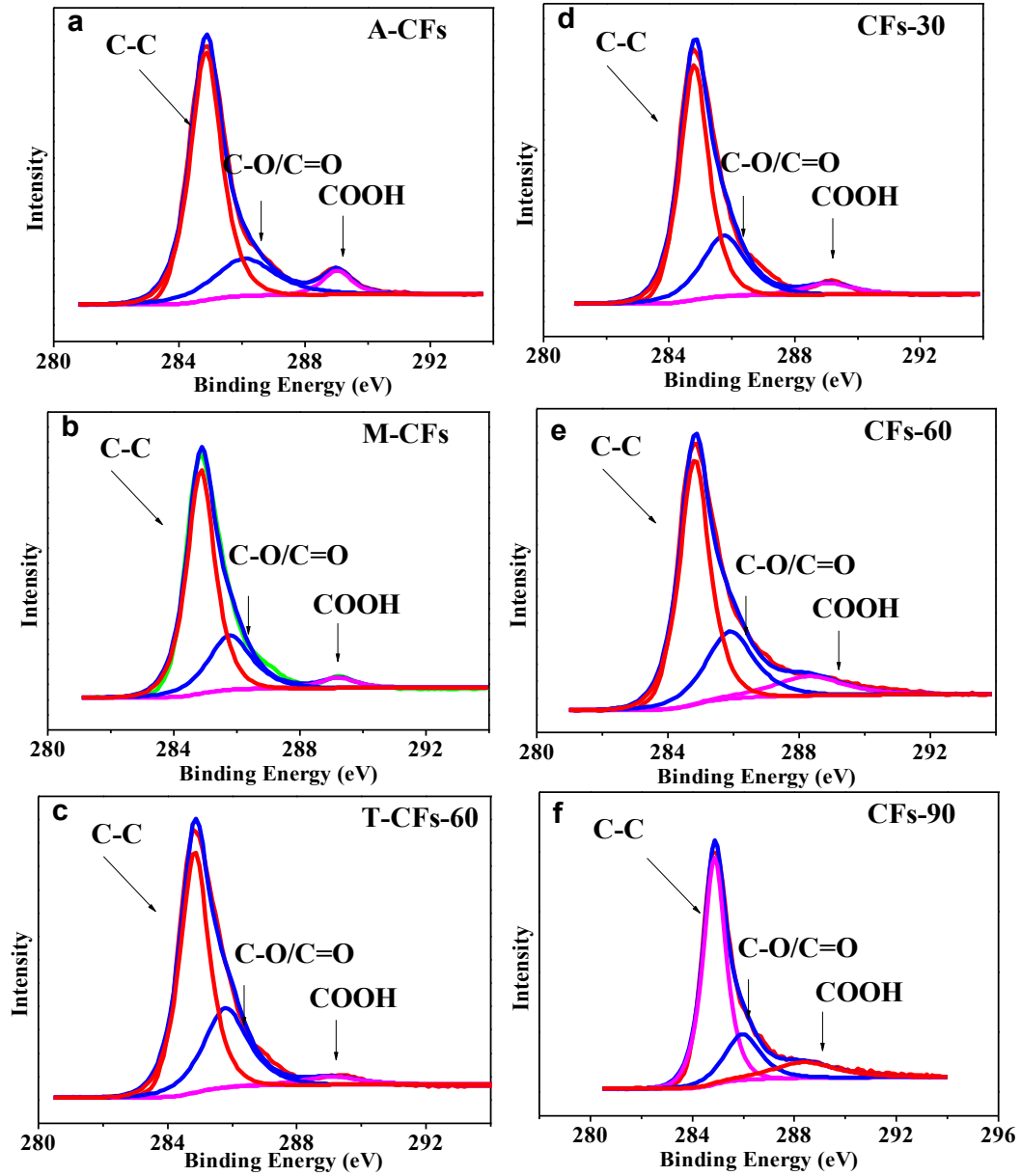


Figure 3. C1s (a, b, c, d, e, f) spectra of A-CFs (a), M-CFs (b), T-CFs-60 (c), CFs-30 (d), CFs-60 (e) and CFs-90 (f)

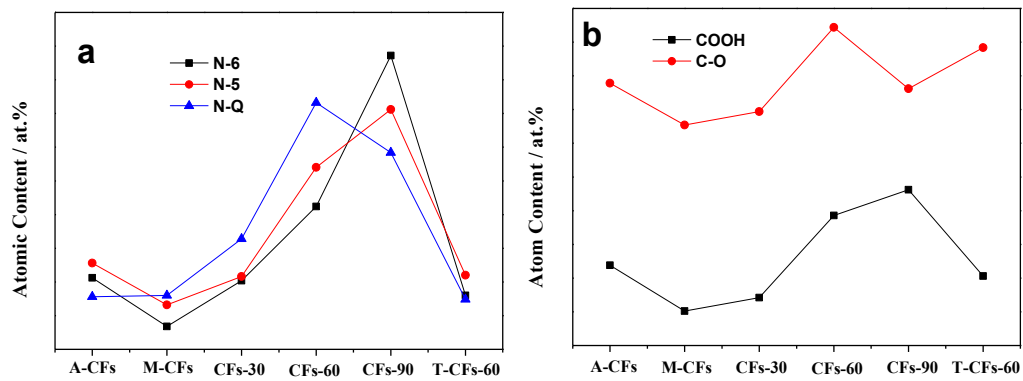


Figure 4. The atomic content of nitrogen species (a) and oxygen species (b) of A-CFs, M-CFs and CFs-30, CFs-60, CFs-90 and T-CFs-60.

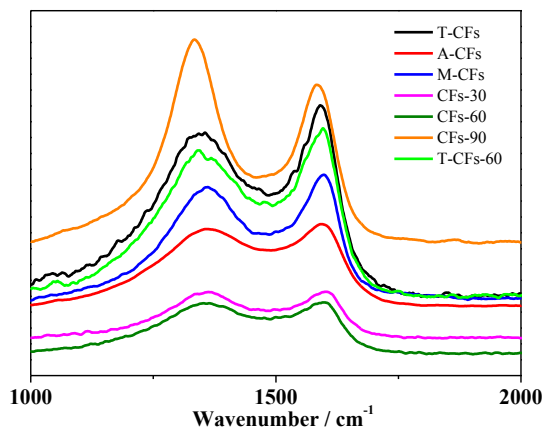


Figure 5. Raman spectra of T-CFs, A-CFs, M-CFs and CFs-30, CFs-60, CFs-90 and T-CFs-60.

on the surface of CFs was removed by the thermal-treatment, and the CFs bundles (Figure 1a) are dismissed to single CFs with the average diameter about 7 μm (insets of Figure 1b and 1c). Formation of single CFs not only increases the specific surface area, but also facilitates the enhancement of functionalization efficiency and capacitive performance. The CFs-60 exhibits almost the same morphology as T-CFs even after acidification, microwave and cold plasma treatment, the morphology of A-CFs, M-CFs, CFs-30 and CFs-90 are just like CFs-60, which are not showed here.

Functional groups are influenced by acidification, microwave and cold plasma treatment, the species and content were measured by XPS. The element content of N, C and O is showed in Table 1. T-CFs has small amount of oxygen groups only. N and O are introduced into T-CFs due to the acidification in mixed HNO_3 and H_2SO_4 acids, especially for oxygen, which increases to 18.38 at.%, the content of N is about 1.79 at.%. To remove the unstable groups, microwave treatment was applied[21]. However, both content of N and O are decreased after microwave treatment. M-CFs has high content of oxygen, but the content of nitrogen is low. To further increase the content of nitrogen, N_2 plasma treatment was applied, which increases from 0.9 at.% to 1.87 at.% after cold plasma treatment for 30 min, 4.23 at.% for 60 min and 5.43 at.% for 90 min. The nitrogen content is higher than the N_2 plasma treated graphene (1.3 at.%) [22], pulsed ion beam treated carbon nanotubes (0.7 - 3.2 at.%) [23], egg derived carbon (2.93 at.%) [24]. It should be mentioned that without acid treatment, the nitrogen content of T-CFs-60 (1.32 at.%) is much less than CFs-60 although the time of plasma treatment is the same. Possibly because acidification creates functional groups on the surface of CFs which is benefit to the doping efficiency of plasma treatment, the mechanism about the role of acidification is under investigation. It is concluded that the combination of acidification and cold plasma treatment plays a significant role in enhancement of the functional groups.

The species and atomic content of nitrogen and oxygen groups were obtained from XPS peak deconvolution, which are showed in Figure 2, Figure 3 and Figure 4, respectively. It is observed that after acidification, the nitrogen species, such as pyridinic N (N-6 at ~ 398.1 eV), pyrrolic N (N-5 at ~ 399.4 eV), quaternary N (N-Q at

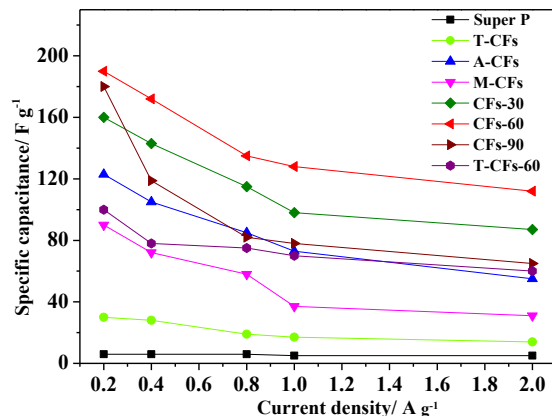


Figure 6. Specific capacitance of Super P, T-CFs, A-CFs, M-CFs, CFs-30, CFs-60, CFs-90 and T-CFs-60 in different current densities

~ 400.4 eV), pyridine N-oxide (N^+-O^- at ~ 404.2 eV), and oxygen species, such as C-O/C=O (hydroxyl, epoxy, alkoxy, carbonyl at ~ 285.7 - 286.3 eV), COOH (~ 288.9 eV) are incorporated into CFs [3,25,26]. The COOH and N^+-O^- groups can improve the supercapacitive performance by improving the wettability, however, the unstable property degrades the cyclic stability [27,28]. During the microwave treatment process, COOH and N^+-O^- groups decreases or even diminishes (Figure 2b), the total content of N decrease, as well as N-5, N-6, N-Q groups. N-5, N-6, N-Q, C-O/C=O and COOH the main functional groups of all CFs except of A-CFs. All the nitrogen species and oxygen species increase after cold plasma treatment, moreover, the content of all species increase with time, except N-Q and C-O of CFs-90.

In Figure 5, the Raman spectra of CFs exhibited two peaks at 1360 cm^{-1} and 1590 cm^{-1} represent the D and G bands, respectively. D band is attributed to a breathing mode of κ -point photons of A_{1g} symmetry, which is related to the defects in graphitic structure. G band arises from an E_{2g} mode which related to the vibration in all sp^2 -bonded carbon atoms [29]. The intensity ratio of D and G band (I_D/I_G) of T-CFs is 0.85, which increase to 0.88 (T-CFs-60) with the plasma treatment for 60 min. After acidification, I_D/I_G of CFs increases from 0.85 to 0.94, due to the increased defects of MWNTs originated from the formation of functional groups. After microwave treatment, the decreasing functional groups results in the decreasing of I_D/I_G (0.91). With prolonging the plasma treatment time to 30 min, 60 min and 90 min, the I_D/I_G increases to 0.98, 1.02 and 1.18, respectively. The phenomenon is due to the variation of functional groups in line with XPS results.

3.2. Electrochemical properties of the CFs

The electrochemical performance of the functionalized CFs are examined by cyclic voltammograms (CVs), galvanostatic charge/discharge and electrochemical impedance spectrum, the results are showed in Figure 6 and Figure 7.

Fig.6 lists the specific capacitance of Super P, T-CFs, A-CFs, M-CFs, CFs-30, CFs-60, CFs-90 and T-CFs-60 at the current density of 0.2 A g^{-1} , 0.4 A g^{-1} , 0.6 A g^{-1} , 1.0 A g^{-1} and 2.0 A g^{-1} . Super P

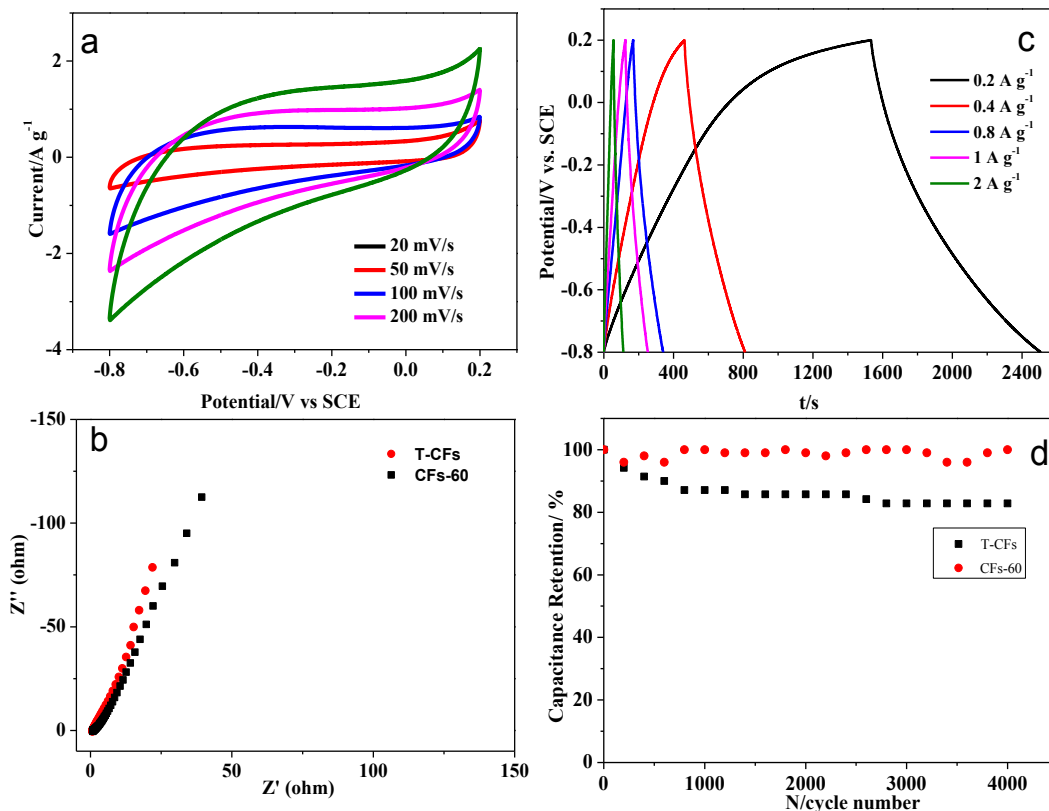


Figure 7. (a): CV plots of CFs-60 at different scan rates, (b): Nyquist plots of CFs-60, the inset is the enlarged Nyquist plots as indicated by the red box (c): Galvanostatic charge/discharge curves of CFs-60 and T-CFs, (d): Cycling stability of CFs-60 and T-CFs.

with low specific capacitance contributes little to the capacitance of CFs. Without functionalization, the specific capacitance of T-CFs is only 30 F g^{-1} at 0.2 A g^{-1} , slightly decreases with the current density increasing. After acidification, the specific capacitance of A-CFs increases significantly, which is 123 F g^{-1} at 0.2 A g^{-1} , while with the increase of current density, the specific capacitance decreases fast, when the current density is 2 A g^{-1} , the specific capacitance is 55 F g^{-1} . The specific capacitance of M-CFs is lower than A-CFs at each current density due to the decrease of functional groups as XPS results show. After 30 min of cold plasma treatment the specific capacitance increases to 172 F g^{-1} at 0.2 A g^{-1} . When increase the treatment time to 60 min, the specific capacitance of CFs-60 reaches to 190 F g^{-1} at 0.2 A g^{-1} and 112 F g^{-1} at 2 A g^{-1} . If the treatment time was elongated to 90 min, the specific capacitance of CFs-90 is 180 F g^{-1} at the current density of 0.2 A g^{-1} , which decrease fast at high current density indicating poor rate performance. CFs-60 has the highest specific capacitance at each current density.

According to the previous reports, N-5, N-6, C=O, C-OH contribute to the specific capacitance [25,30]. N-6 and N-Q improved the conductivity of carbon materials [31], which is affected by oxygen groups, especially the unstable COOH and N^+-O^- groups negatively. Both of nitrogen and oxygen groups influence the rate performance and long life stability together. The above results showed that, except CFs-90, the order of specific capacitance is similar to

that of functional groups content, which demonstrates that increasing the content of functional groups is benefit to the enhancement of specific capacitance. While for CFs-90, the total content of nitrogen and oxygen (COOH) is higher than that of CFs-60, the content of C-O and N-Q is lower than that of CFs-60, which is possibly detrimental to the conductivity and specific capacitance resulting in poor rate performance and stability, so we choose 60 min as the optimized time of cold plasma treatment. Compared to T-CFs-60, CFs-60 with larger amount of functional groups exhibit higher specific capacitance, demonstrating that acidification before cold plasma treatment is an important process for enhancement of specific capacitance.

Figure 7 shows the CVs, galvanostatic charge/discharge curves, Nyquist plots and cycling stability of CFs-60. Figure 7a shows the cyclic voltammograms (CVs) of CFs-60 at different scan rates. The asymmetry of CV curves with respect to potential axis is attributed to the pseudo-faradaic processes on the surface involving surface nitrogen and oxygen functional groups [32]. It can be seen that the response current density increase with scan rate increasing, indicating a good rate capability of CFs-60. The rapid electrochemical process should be related to the modest electronic conductivity and little charge transfer resistance (R_{ct}). The obtained Nyquist plot in the frequency range of 0.01-10000 with AC signal amplitude of 5 mV is displayed in Figure 7b. The plot of CFs-60 which is similar to T-CFs does not show semicircle regions, probably due to the low

faradaic resistance of the materials. Figure 7c shows the charge/discharge curves of CFs-60 at various current densities from 0.2 A g⁻¹ to 2.0 A g⁻¹, the specific capacitance are calculated from these curves. All curves exhibit triangle shape with nonlinearity reveals representative pseudocapacitive behavior of CFs-60, resulting from the electrochemical adsorption/desorption and/or redox reactions at the electrode-electrolyte interface. The cyclic stability of CFs-60 and T-CFs was measured by galvanostatic charge/discharge. The specific capacitance retention of the continuous 4000 cycles is showed in Figure 7d. Due to the extremely low content of functional groups, the specific capacitance of T-CFs remains unchanged during the repeating charge and discharge process with the specific retention around 100%. CFs-60 with large amount of functional groups still has the specific retention of 83% at the end of 4000 cycles, indicating good long life stability of CFs-60.

4. CONCLUSIONS

In summary, nitrogen and oxygen co-doped carbon fibers are prepared by acidification and N₂ cold plasma treatment, and acidification can promote the enhancement of nitrogen content introduced by cold plasma. The incorporated nitrogen and oxygen species increase the specific capacitance of CFs significantly, and higher content of functional groups results in higher specific capacitance. CFs-60 functionalized by acidification and N₂ cold plasma for 60 min has high specific capacitance, good rate capability and stability.

5. ACKNOWLEDGEMENT

This work was supported by Guangxi Natural Science Foundation(No. 2015GXNSFBA139220 and 2016GXNSFAA380107) and the funding from Collaborative Innovation Center for Exploration of Hidden Nonferrous Metal Deposits and Development of New Materials in Guangxi, Guangxi Key Laboratory of Processing for Non-ferrous Metal and Featured Materials.

REFERENCE

- [1] J. Yan, T. Wei, B. Shao, et al., Carbon, 48, 487 (2010).
- [2] M. K. Liu, S. X. He, Y. E. Miao, et al. RSC Adv., 5, 55109 (2015).
- [3] Z. H. Luo, L. H. Zhu, Y. F. Huang, et al. Synth. Met., 175, 88 (2013).
- [4] L. S. Zhang, Q. W. Ding, Y. P. Huang, et al., ACS Appl. Mater. Interfaces, 7, 22669 (2015).
- [5] B. Xu, S. F. Yue, Z. Y. Sui, et al., Sci., 4, 2826 (2011).
- [6] H. L. Guo, P. Su, X. F. Kang, et al., J. Mater. Chem. A, 1, 2248 (2013).
- [7] H. M. Jeong, J. W. Lee, W. H. Shin, et al., Nano Lett., 11, 2472 (2011).
- [8] V. H. Pham, S. H. Hur, E. J. Kim, et al., Chem. Commun., 49, 6665 (2013).
- [9] J. H. Yang, M. R. Jo, M. Kang, et al., Carbon, 73, 106 (2014).
- [10] Z. Y. Sui, Y. N. Meng, P. W. Xiao, et al., ACS Appl. Mater. Interfaces, 7, 1431 (2015).
- [11] O. Y. Podyacheva, S. V. Cherepanova, A. I. Romanenko, et al., Carbon, 122, 475 (2017).
- [12] Z. H. Luo, M. Zhu, Y. Z. Zhao, et al., J. New Mater. Electrochem. Systems, 20, 95 (2017).
- [13] X. Q. Yang, C. F. Li, R. W. Fu, J. Power Sources, 319, 66 (2016).
- [14] X. Q. Yang, H. Ma, G. Q. Zhang, Langmuir, 33, 3975 (2017).
- [15] X. Q. Yang, J. L. Yu, W. J. Zhang, et al., RSC Adv., 7, 15096 (2017).
- [16] X. W. Wang, G. Z. Sun, P. Routh, et al., Chem. Soc. Rev., 43, 7067 (2014).
- [17] S. H. Park, J. Chae, M. H. Cho, et al., J. Mater. Chem. C, 2, 933 (2014).
- [18] F. Poncin-Epaillard, J. C. Brosse, T. Falher, Macromolecules, 30, 4415 (1997).
- [19] V. K. Abdelkader, S. Scelfo, C. Garcia-Gallarín et al., J. Phys. Chem. C, 117, 16677 (2013).
- [20] O. Chirila, M. Totolin, G. Cazacu, Ind. Eng. Chem. Res., 52, 13264 (2013).
- [21] K. H. Lee, J. Oh, J. G. Son, et al., ACS App. Mater. Interfaces, 6, 6361 (2014).
- [22] Y. Wang, Y. Y. Shao, D. W. Matson, et al., ACS Nano, 4, 1790 (2010).
- [23] P. M. Korosenko, V. V. Bolotov, S. N. Nesov et al., Nucl. Instrum. Meth. Phys. Res. B, 358, 131 (2015).
- [24] J. Zhang, S. Y. Wu, X. Chen, et al., J. Power Sources, 271, 522 (2014).
- [25] W. Fan, Y. Y. Xia, W. W. Tjiu, et al., J. Power Sources, 243, 973 (2013).
- [26] A. Ganguly, S. Sharma, P. Papakonstantinou, et al., J. Phys. Chem. C, 115, 17009 (2011).
- [27] Z. L. Lin, Y. Liu, Y. G. Yao, et al., J. Phys. Chem. C, 115, 7120 (2011).
- [28] M. Vujković, N. Gavrilov, I. Pašti, Carbon, 64, 472 (2013).
- [29] Z. H. Luo, L. H. Zhu, Y. F. Huang et al., Synth. Met., 175, 88 (2013).
- [30] N. P. Subramanian, X. Li, V. Nallathambi et al., J. Power Sources, 188, 38 (2009).
- [31] H. Y. Liu, H. H. Song, X. H. Chen, J. Power Sources, 285, 303 (2015).
- [32] C. Moreno-Castilla, M. B. Dawidzauk, Carbon, 50, 3324 (2009).